ORIGINAL RESEARCH

Multipotent Myoepithelial Progenitor Cells Are Born Early during Airway Submucosal Gland Development

Preston J. Anderson[1,2,3], Thomas J. Lynch[1], and John F. Engelhardt[1]

[1]Department of Anatomy and Cell Biology, University of Iowa, Iowa City, Iowa; [2]Iowa Biosciences Academy, Iowa City, Iowa; and [3]Iowa Center for Research by Undergraduates, Iowa City, Iowa

Abstract

Airway submucosal glands (SMGs) are facultative stem cell niches for the surface epithelium, but the phenotype of the SMG-derived progenitor cells remains unclear. In other organs, glandular myoepithelial cells (MECs) have been proposed to be multipotent progenitors for luminal cells. We sought to determine the developmental phase during which mouse tracheal glandular MECs are born and whether these MECs are progenitors for other cell phenotypes during SMG morphogenesis. To approach this question, we localized two MEC protein markers (α-smooth muscle actin [αSMA/*ACTA2*] and smooth muscle myosin heavy chain 11 [SMMHC/*MYH11*]) during various stages of SMG development (placode, elongation, branching, and differentiation) and used *ACTA2*-Cre^{ERT2} and *MYH11*-Cre^{ERT2} transgenic mice to fate map MEC-derived lineages during SMG morphogenesis. Both αSMA- and SMMHC-expressing cells emerged early after placode formation and during the elongation phase of SMG development. Lineage tracing in newborn mice demonstrated that lineage-positive MECs are born at the tips of invading tubules during the elongation phase of gland development. Lineage-positive MECs born within the first 7 days after birth gave rise to the largest percentage of multipotent progenitors capable of contributing to myoepithelial, serous, mucous, and ductal cell lineages. Serial tamoxifen-induction of both Cre-driver lines demonstrated that lineage-positive multipotent MECs contribute to ∼ 60% of glandular cells by 21 days after birth. In contrast, lineage-traced MECs did not contribute to cell types in the surface airway epithelium. These findings demonstrate that MECs born early during SMG morphogenesis are multipotent progenitors with the capacity to differentiate into other glandular cell types.

Keywords: submucosal glands; stem cells; myoepithelial cell; development; trachea

Clinical Relevance

Submucosal glands are secretory structures in the proximal cartilaginous airways and are adversely affected in many hypersecretory lung diseases including cystic fibrosis, chronic bronchitis, and asthma. Although submucosal glands are known to be a stem cell niche in the proximal airway, little is known about how this niche is established during development and the phenotype of glandular progenitor cells. Using lineage tracing, we demonstrate that myoepithelial cells born early during glandular morphogenesis contribute to multiple lineages of the mature gland.

Airway submucosal glands (SMGs) are secretory structures found in the submucosa of large conducting airways and form a contiguous epithelium with the airway surface. SMGs in mice are limited to the proximal trachea, but in humans they are found throughout all levels of the cartilaginous airways. SMGs play important roles in airway innate immunity and secrete the majority of fluid, mucus, and antimicrobials into the large airways of most species (1, 2). In mice, multipotent stem cells have been shown to exist within SMGs and to contribute to regeneration of the surface airway epithelium (SAE) after

(Received in original form September 26, 2016; accepted in final form January 4, 2017)

This work was supported by National Institutes of Health grants DK047967 (J.F.E.), the University of Iowa Center for Gene Therapy (DK54759) (J.F.E.), National Ferret Research and Resource Center (R24 HL123482) (J.F.E.), and the Carver Chair in Molecular Medicine (J.F.E.).

Author Contributions: Conception and design: P.J.A., T.J.L., and J.F.E.; performed experiments: P.J.A.; analysis and interpretation: P.J.A., T.J.L., and J.F.E.; and drafting the manuscript: P.J.A. and J.F.E.

Correspondence and requests for reprints should be addressed to John F. Engelhardt, Ph.D., Department of Anatomy and Cell Biology, University of Iowa, Room 1-111 Bowen Science Building, 51 Newton Road, Iowa City, IA 52242-1009. E-mail: john-engelhardt@uiowa.edu

This article has an online supplement, which is accessible from this issue's table of contents at www.atsjournals.org

Am J Respir Cell Mol Biol Vol 56, Iss 6, pp 716–726, Jun 2017

Originally Published in Press as DOI: 10.1165/rcmb.2016-0304OC on January 26, 2017
Internet address: www.atsjournals.org

severe injury (3–7). In diseases such as cystic fibrosis, asthma, chronic bronchitis, and other forms of chronic obstructive lung disease, SMG hypertrophy can lead to excessive or altered mucus production in the airway (2, 8, 9), and these changes can also alter properties of the SMG stem cell niche (10).

Fully developed SMGs are composed of ciliated ducts, collecting ducts, mucous tubules, and serous tubules. The cellular composition of ciliated ducts is similar to that of the surface airway epithelium and primarily includes basal and ciliated cells. Lysozyme-expressing serous cells and mucus-secreting cells are generally considered to be differentiated cell types that emerge later during SMG morphogenesis and line the serous and mucous tubules, respectively. Collecting ducts are composed of a nonciliated columnar cell type of poorly defined phenotype. Myoepithelial cells (MECs) line the outside of tubules within SMGs and express both alpha-smooth muscle actin (αSMA) and smooth muscle myosin heavy chain 11 (SMMHC).

Despite a large body of literature enhancing our understanding of progenitor cells on the airway surface (11), there is fairly little known about the lineage relationships of SMG progenitors. The ducts of airway SMGs have historically been considered the sites at which SMG stem cells reside, based on the discovery of slowly cycling nucleotide label-retaining cells in this region and the existence of duct progenitors that are multipotent for SAE cell types (3–5, 12, 13). However, others have found that glandular label-retaining cells, which are able to cycle after repeated injury and to retain multiple nucleotide labels, can reside deeper within SMG tubules (6, 7, 10). Furthermore, isolated progenitors from mouse SMGs are multipotent for both glandular and surface airway epithelial cell types and have a greater regenerative capacity than SAE progenitors (6). These studies emphasize an increased need to understand the progenitor cell phenotypes in SMGs.

The majority of mouse models used to study airway stem cells rely on injury to induce proliferation and cellular expansion (14) because of the low turnover rate of airway epithelia (15). However, the field has also learned a significant amount about glandular stem cells by studying the earliest phases of SMG morphogenesis (16, 17). In this context, SMG placodes, which are composed of primordial glandular stem cells, use Wnt signals to coordinate early stages of gland development and branching morphogenesis (18–23). Wnt signaling in adult mouse SMGs also appears to be a component of the stem cell niche, with slowly cycling label-retaining cells residing near glandular regions of increased Wnt signaling in myoepithelial and serous cells (6). Interestingly, after severe airway injury, the first cycling SMG progenitors activate expression of two transgenic Wnt reporters that are also activated in primordial glandular stem cells during the placode phase of SMG morphogenesis (6). Thus, regenerative aspects of the adult glandular stem cell niche may share biologic processes involved in glandular stem cell niche formation.

Lineage relationships during glandular morphogenesis have been most extensively studied in the mammary gland. In this context, the mammary gland MEC is considered to be a candidate multipotent stem cell that is closely related to the luminal basal cell (24–27). Interestingly, lineage tracing studies using the *ACTA2-Cre*^{ERT2} driver have demonstrated that mouse mammary MECs are long-lived, lineage-restricted progenitors of basal cells during pregnancy *in vivo*, but have the capacity to form all cellular components of the mammary gland when transplanted *ex vivo* (26). Similarly, MECs of the lacrimal gland have also been suggested to have multipotent capacity for differentiation during development and repair after injury (28, 29).

Given the conserved stem cell biology during development of SMGs and regenerative expansion of adult SMG progenitors after injury (6, 7), and the fact that MECs in other glandular organs are thought to be multipotent stem cells, we sought to investigate when the MEC lineage is established during airway SMG morphogenesis. Using *ACTA2*-Cre^{ERT2} and *MYH11*-Cre^{ERT2} lineage tracing, we demonstrate that airway glandular MECs are born early during SMG development and have multipotent capacity for other glandular lineages.

Materials and Methods

Animals

All animal experimentation was performed according to protocols approved by the Institutional Animal Care and Use Committees of the University of Iowa. The mouse Cre reporter strain Gt(ROSA)26Sor$^{tm4(ACTB-tdTomato,-EGFP)Luo}$ (ROSA-TG) (30) and MEC Cre-driver strain Tg(Myh11-cre/ERT2)1Soff (*MYH11-Cre*^{ERT2}) (31) were purchased from Jackson Laboratory (Bar Harbor, ME). After Cre-mediated recombination, ROSA-TG mice switch expression from a membrane-associated tdTomato to a membrane-associated EGFP. A second Cre-driver strain of mice Tg(Acta2-cre/ERT2)51Pcn (*ACTA2-Cre*^{ERT2}) was also used (32). Both male and female *ACTA2*-Cre^{ERT2}:ROSA-TG double-transgenic mice were evaluated. Only male *MYH11-Cre*^{ERT2}:ROSA-TG were used because the *MYH11-Cre*^{ERT2} transgene is on the Y-chromosome. Newborn ferret tracheas were obtained from the Iowa National Ferret Research and Resource Center.

Lineage Tracing Studies and Tissue Harvesting

Cre-mediated recombination was induced using a single injection (intraperitoneal) of tamoxifen suspended in corn oil (0.2 mg/dose for pups; 2 mg/kg for adults) or by serial gavages (0.2 mg/dose) every other day from birth to 18 days of age. Tracheas were harvested at various points up to 21 days, fixed in 4% paraformaldehyde at 4°C for 48 hours, and then embedded in optimal cutting temperature compound.

Histology, Immunofluorescent Localization, and Imaging

Frozen sections (8 μm) were postfixed in 4% paraformaldehyde for 20 minutes, washed in PBS, and then incubated in blocking buffer (PBS, 20% donkey serum, 0.3% Triton X-100, and 1 mM $CaCl_2$) for 1 hour. The primary antibodies, lectins, and dilutions used are indicated in Table E1 in the online supplement. Primary antibodies were applied to sections in blocking buffer containing 1% donkey serum overnight at 4°C. Slides were then washed in PBS and stained with secondary antibodies for 2 hours at room temperature (Table E1). When paraffin sections were used (Lef-1 and Sox9 staining), antigen retrieval was performed after deparaffinization by boiling in citrate buffer for 5 minutes in a pressure cooker. The sections were then processed as described earlier. For lectin staining, frozen sections were first blocked with an Avidin/Biotin Blocking Kit (Vector Laboratories SP-2001) and then

rinsed in PBS before incubation with the biotinylated-lectin and avidin-conjugated-fluorochrome, sequentially, for 30 minutes each. Slides were washed in PBS and then stained using 4′,6-diamidino-2-phenylindole. Slides were mounted with ProLong Gold (P36930; Invitrogen, Carlsbad, CA). Fluorescent images were collected with a Zeiss LSM 700 line-scanning confocal microscope (Carl Zeiss, Göttingen, Germany), and images were processed using Fiji-ImageJ.

Morphometric Analysis

All images were acquired with the same scope settings to ensure scales and thresholds were the same. The area of SMG structures was quantified using the area tool of ImageJ. Image analysis for the lineage tracing green fluorescent protein (GFP) reporter and cell type markers was performed using the MetaMorph Software's (Nashville, TN) Multi Wavelength Cell Scoring application with at least three sections 50 μm apart, evaluated for each animal. These values were averaged for animal/trachea and the N animals used to calculate means and SEM.

Gland Development Nomenclature and Definitions

We described our findings in the context of four phases of SMG development: phase 1 (placode): primordial gland placodes form in the SAE with no visible lumen; phase 2 (elongation), invagination of SMG buds with the formation of a lumen; phase 3 (branching), growing primary tubules begin to branch; phase 4 (differentiation), maturation of SMG mucous and serous tubules with differentiated phenotypes.

Results

MEC Phenotypes Emerge Very Early during Airway SMG Development

To evaluate the stage of SMG morphogenesis during which MECs are born, we localized two phenotypic markers (αSMA and SMMHC) of mature MECs during postnatal tracheal development in the mouse (Figure 1). During phase 1 of SMG morphogenesis at 0–3 days of age, epithelial αSMA expression was not observed in the placode and early invaginating buds (Figure 1A). In contrast, during elongation (phase 2) and early branching (phase 3), αSMA expression began to emerge on the periphery of tubules with visible lumens by 3–5 days of age (Figures 1B and 1C). By 21 days after birth, αSMA expression was observed around nearly all tubules (Figure 1D). A very similar developmental pattern of expression was also observed using immunofluorescent staining for SMMHC as a marker for MECs (Figures 1E–1H).

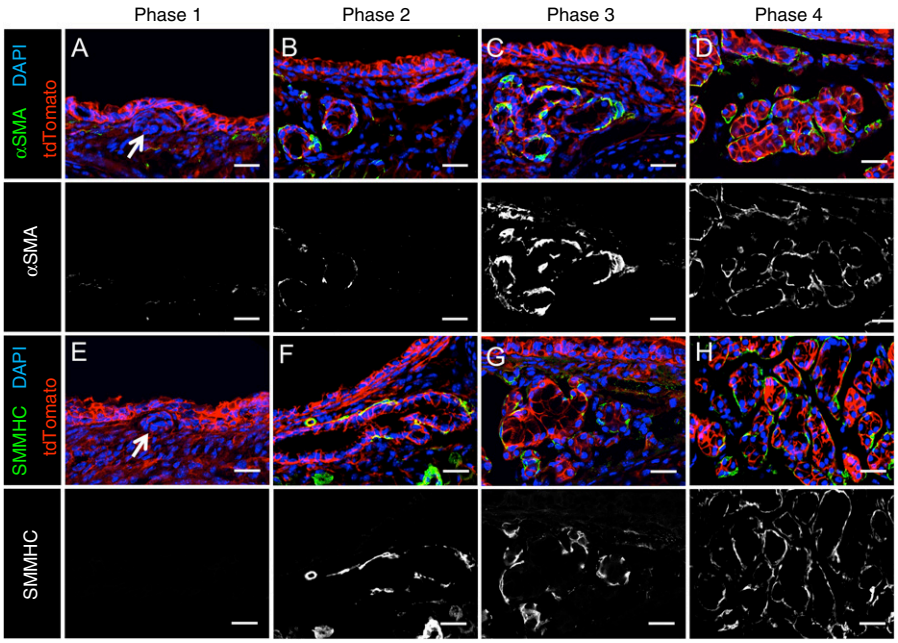

Figure 1. α-Smooth muscle actin–positive (αSMA^+) and smooth muscle myosin heavy chain 11–positive ($SMMHC^+$) cells emerge during the elongation phase of submucosal gland (SMG) morphogenesis. Gt(ROSA)26Sor$^{tm4(ACTB-tdTomato,-EGFP)Luo}$ (ROSA-TG) mice were harvested at 3, 5, 7, and 21 days after birth. Tracheal sections were immunofluorescently stained for (*A–D*) αSMA or (*E–H*) SMMHC. Representative images for each stain were taken for placode (phase 1), elongation (phase 2), branching (phase 3), and differentiation (phase 4) phases of SMG development. Single-channel images of αSMA and SMMHC are below each of the merged panels. *Arrows* in *A* and *E* mark the glandular placode. *Scale bars*: 25 μm.

The Lef-1 transcription factor is highly expressed in early SMG progenitors during the placode and elongation phases (20) and is required for SMG development (i.e., Lef-1 knockout mice fail to develop SMGs) (18, 19, 21). Mammary glands also require Lef-1 for development (33, 34). Interestingly, Sox9 is also required for mammary gland morphogenesis, and lineage tracing studies demonstrate that $Sox9^+$ mammary progenitor cells give rise to both luminal and myoepithelial lineages (35). However, Sox9 is only required for lineage commitment and proliferation of luminal, but not myoepithelial, cells of the mammary gland (35). To better understand the phenotype of early αSMA^+ progenitors during SMG development, we colocalized Lef-1 and Sox9 with αSMA. In addition to mouse trachea, we also evaluated newborn ferret trachea, as this species has abundant tracheal SMG placodes at birth (22). Lef-1 and Sox9 were highly expressed in epithelial cells of the placode, and αSMA^+ cells were absent in both species at this stage (Figure E1). During the elongation phase, αSMA^+ cells emerged at the periphery of tubules in both species, and a subset of these cells was positive for Lef-1 and Sox9 (Figure E1). These findings suggest that MECs born early during SMG development partially retain the phenotype of luminal progenitors, and thus MECs may be daughters of early luminal cells.

Lineage Tracing Demonstrates Early MEC Progenitors Dynamically Expand during Glandular Morphogenesis

To confirm the phases in which MEC arise during gland development and to evaluate whether early MEC lineages are multipotent, we performed lineage tracing with an *ACTA2*-Cre^{ERT2} driver on a ROSA-TG Cre-reporter background. This *ACTA2*-Cre^{ERT2} driver marked only SMG MECs in adult mice after tamoxifen injection (Figure E2). Reasoning that the

birth of MECs occurs within the first few days of SMG morphogenesis, we injected newborn pups (<1 day old) with tamoxifen and harvested tracheas at 3, 5, 7, and 21 days after injection (Figure 2A). Results from these experiments demonstrated rapid labeling of tracheal smooth muscle and vascular smooth muscle throughout all postnatal points (Figure E3). In the most proximal trachea, where gland formation first initiates, GFP^+ cells surrounding tubules with visible lumens were observed at 3 and 5 days postbirth (Figures 2B and 2C). By 7–21 days after birth, lineage-traced GFP^+ cells marked both cells of glands consistent with MEC morphology and cells morphologically resident in the lumen of tubules and ducts (Figures 2D and 2E). Overall, *ACTA2*-Cre^{ERT2} lineage tracing did not mark the earliest placode phase (Figures 2F and 2J), but did trace cells at the tips of early-formed tubules during the elongation phase (Figures 2G and 2J).

During the branching and differentiated phases of gland development, lineage-traced cells were observed with apical membranes that reached the lumen of tubules, as well as surrounding the basement membrane of tubules with morphology consistent with MECs (Figures 2H–2J). This finding suggests that MECs born early during gland morphogenesis may differentiate into other phenotypic lineages within SMGs.

Lineage-Traced MECs Express Basal Cell Markers during All Phases of Glandular Morphogenesis

Lineage tracing during development comes with caveats that relate to promoter specificity of the Cre-driver. For example, during the elongation phase of SMG morphogenesis, it is possible that the *ACTA2* promoter is ectopically expressed in undifferentiated progenitors. Although this limitation of lineage tracing is difficult to completely disprove, one approach to support specificity of the Cre-driver is to localize other phenotypic markers of the cell type being mapped. MECs are thought to be phenotypically very similar to basal cells in multiple organs. Three common basal cell markers include p63, CK5, and CK14 (36), and these markers are also expressed in all or a subset of MECs in mature SMGs (5, 6). To this end, we colocalized GFP expression with p63, CK5, or CK14 during all phases of gland development in animals that were pulsed with tamoxifen at birth. Results from these experiments demonstrated that many of the *ACTA2*-Cre^{ERT2} lineage-traced cells also expressed p63, CK5, and CK14 during all phases of gland development in which lineage traced cells were observed (Figure 3). During phase 1 (placode phase), all three basal cell markers were expressed in the absence of lineage-traced cells (Figures 3A–3C). During phase 2 (elongation phase),

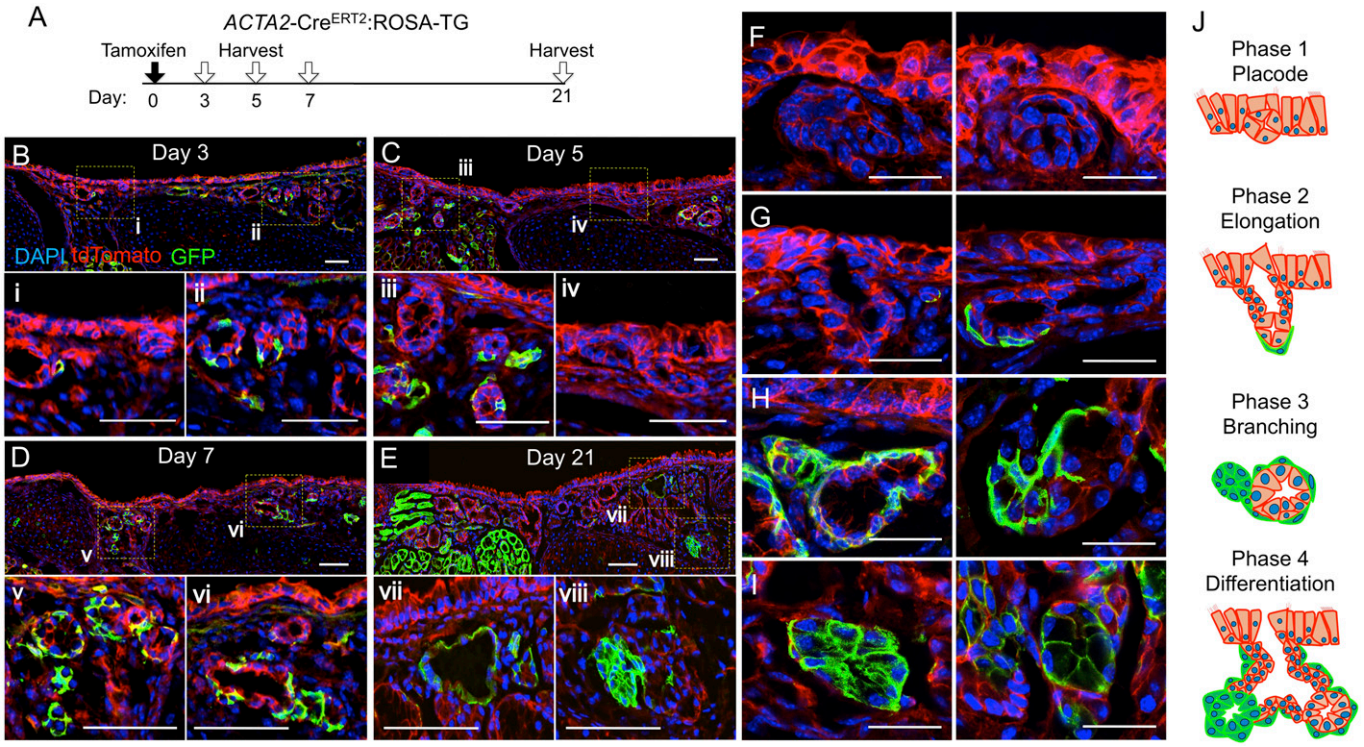

Figure 2. α-Smooth muscle actin (*ACTA2*)-Cre^{ERT2} lineage tracing of myoepithelial cells during submucosal gland development. (*A*) Myoepithelial cell lineage tracing timeline. Newborn *ACTA2*-Cre^{ERT2}:ROSA-TG mice were treated with a single injection of tamoxifen (0.2 mg) on the day of birth, and mice were then harvested on 3, 5, 7, and 21 days of age. (*B–E*) Representative photomicrographs show GFP and tdTomato expression in trachea sections at the indicated ages. DAPI was used to mark nuclei. Boxed regions (*i–viii*) are enlarged below the main panels. (*F–I*) Representative images are shown for the various phases of gland development, including (*F*) placode phase (phase 1), (*G*) elongation phase (phase 2), (*H*) branching phase (phase 3), and (*I*) differentiation phase (phase 4). Two different stages of the elongation phase are shown in (*G*), depicting a GFP-negative early-stage (*left*) and GFP-positive later-stage (*right*) tubule based on size. (*J*) Schematic diagram of the various phases of gland development shown in (*F–I*). *Green cells* mark lineage contribution observed using the *ACTA2*-Cre^{ERT2} driver. *Scale bars*: *B–E*, 50 μm; *F–I*, 25 μm.

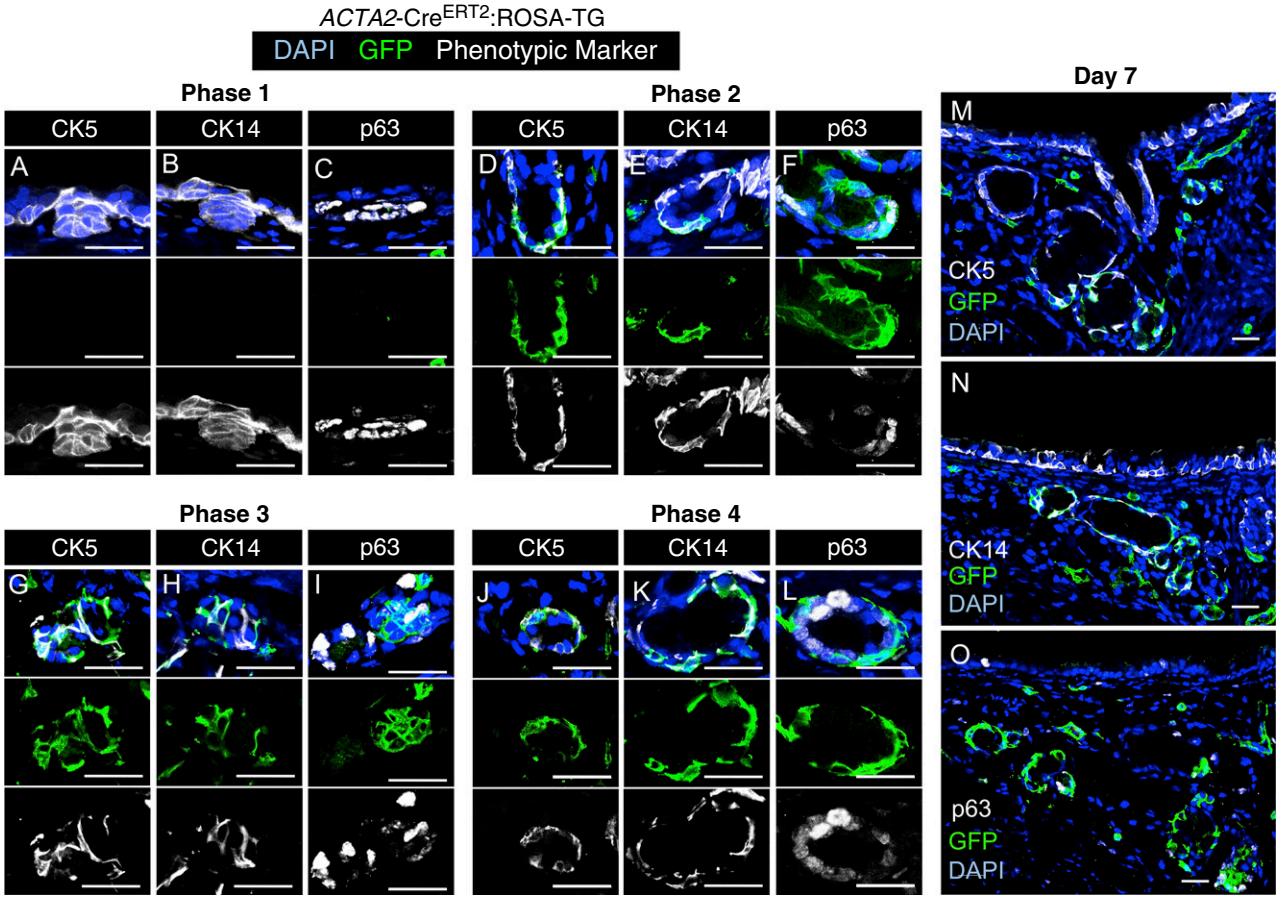

Figure 3. *ACTA2*-Cre^{ERT2} lineage-traced myoepithelial cells express basal cell markers early during submucosal gland development. *ACTA2*-Cre^{ERT2}:ROSA-TG mice were induced on the day of birth (0.2 mg) and harvested at 3, 5, 7, or 21 days of age. Tracheal sections for the four phases of gland development were immunostained for GFP, CK5, CK14, and/or p63. This procedure required antigen retrieval, which prevented the immunodetection of tdTomato. DAPI was used to mark nuclei. (*A–C*) Placode phase (phase 1), (*D–F*) elongation phase (phase 2), (*G–I*) branching phase (phase 3), and (*J–L*) differentiation phase (phase 4). Multichannel images are shown above single-channel images for each phase. (*M–O*) Low-power images of 7-day tracheal sections stained for each of the markers, as indicated. *Scale bars*: 25 μm.

most lineage-traced cells expressed CK5 and CK14, whereas a subset of cells at the tips of the tubules expressed p63 (Figures 3D–3F). Similar patterns of expression were observed during phase 3 (branching phase) and phase 4 (maturation phase) (Figures 3G–3O). These findings support the notion that early during gland development, newly born MECs retain a basal cell phenotype that is similar to that of primordial glandular stem cells found in the placode and that this phenotype is also retained in more mature MECs.

MEC Progenitors Give Rise to Other Glandular Cell Types during Development

To conclusively demonstrate that *ACTA2*-Cre^{ERT2} lineage-traced cells give rise to non-MEC lineages during SMGs morphogenesis, we evaluated the abundance of αSMA-positive and αSMA-negative glandular cells that expressed the GFP lineage marker (Figure 4). By 21 days postinduction, GFP expression was observed in luminal cells of tubules that lacked αSMA expression (Figure 4A). During early stages of gland development, tubules containing lineage-tagged αSMA-negative cells often lacked lumens, whereas during later stages of gland maturation, clear lumens could be observed (Figure 4B). At 3 days postinduction, ∼50% of αSMA$^+$ cells were also GFP-positive; this fraction declined to 25% by Day 21 (Figure 4C). This finding reflects two important points: First, a single injection of tamoxifen at birth was only effective in labeling half of the MECs born by 3 days of age, and second, ∼50% of MECs likely emerge after clearance of tamoxifen from newborn animals, based on the ∼50% drop in lineage tracing efficiency by 21 days of age. However, the percentage of GFP$^+$ cells that also expressed αSMA was 93% at Day 3 (Figure 4D); this demonstrated specificity of the *ACAT2*-Cre^{ERT2} driver, given that the percentage is well within the limits of morphometry for colocalization of two proteins in different cellular compartments (i.e., membrane-bound GFP and cytoplasmic αSMA). Interestingly, the percentage of GFP$^+$ cells that also expressed αSMA$^+$ declined to 67% at Day 21 postinduction (Figure 4D). Looking at these data an alternative way, the percentage of GFP$^+$ cells that lacked αSMA expression rose significantly ($P < 0.0001$) by fivefold between 3 and 21 days postlabeling (Figure 4E),

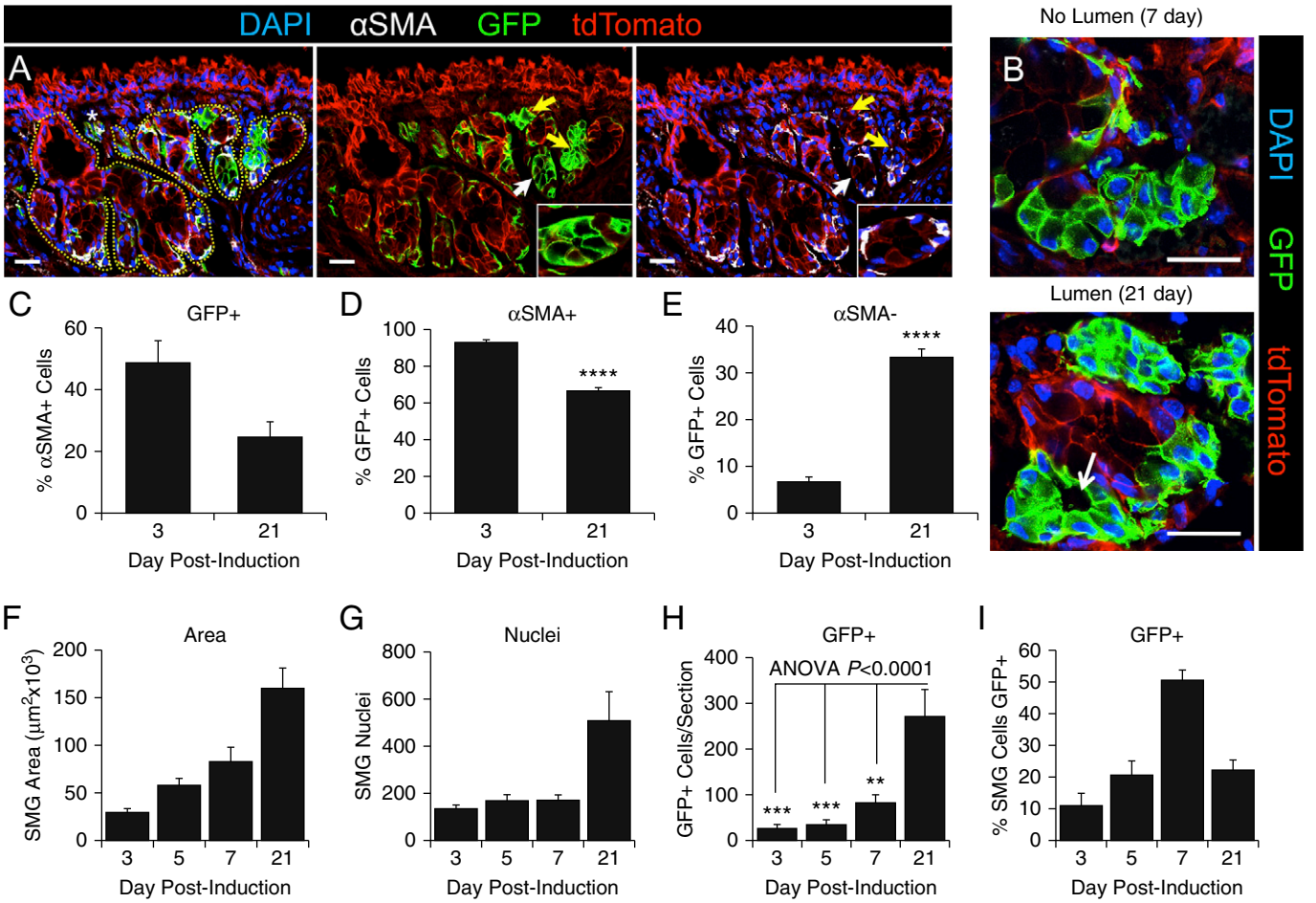

Figure 4. Quantitative analysis of *ACTA2*-Cre^{ERT2}-mediated GFP expression during submucosal gland development. (*A*) *ACTA2*-Cre^{ERT2}:ROSA-TG mice were induced on the day of birth, and 21-day-old tracheal samples were then immunofluorescently evaluated for GFP, αSMA, and tdTomato expression. DAPI was used to mark nuclei. The glandular epithelium is marked by a *yellow dashed line* in the panel on the *left* and is an example of regions quantified for various endpoints. The *asterisk* in the *left* panel marks a vessel that is excluded from the quantification. *Arrows* mark GFP$^+$ tubules, with the *white arrow* indicating the region of the inset in the *right* two panels. (*B*) Two examples of GFP$^+$ SMG tubules without and with a visible lumen, during branching and differentiation phases, respectively. (*C*) The percentage of αSMA$^+$ glandular cells that were also GFP$^+$ at 3 and 21 days postinduction. (*D*) The percentage of GFP$^+$ glandular cells that were also αSMA$^+$. (*E*) The percentage of GFP$^+$ glandular cells that did not express αSMA. (*F–I*) SMGs were quantified for (*F*) total area, (*G*) number of nuclei, (*H*) number of GFP$^+$ cells per section, and (*I*) the percentage of SMG cells staining positive for GFP. Data depict the mean ± SEM of $n = 4$–8 mice from multiple sections >50 μm apart. *Asterisks* denote significance levels using (*D* and *E*) two-tailed Student's *t* test or (*H*) one-way ANOVA with Bonferroni's post-test: $^{**}P < 0.01$; $^{***}P < 0.001$; and $^{****}P < 0.0001$. *Scale bars*: 25 μm.

demonstrating commitment of MECs to other glandular lineages during development. The differentiation of MECs to other glandular cell types correlated with the growth and differentiation of SMGs, as indicated by increased area and number of cells within glands (Figures 4F and 4G). In support of an expanding MEC progenitor cell population, the number of *ACAT2*-Cre^{ERT2} lineage-tagged GFP$^+$ cells significantly expanded 10-fold ($P < 0.001$) between 3 and 21 days postlabeling (Figure 4H). Interestingly, the percentage of cells within glandular regions that were GFP$^+$ peaked at 7 days postlabeling and then declined at 21 days (Figure 4I). This peak was not a result of a transient rise in GFP$^+$ cells with the inability to self-renew, given the overall rise in the abundance of lineage-traced cells with time postlabeling (Figure 4H). We interpret this transient rise in the percentage of lineage-tagged SMG cells (Figure 4I) to suggest that either lineage-positive or lineage-negative progenitors born later during SMG development contribute to a larger fraction of glandular epithelia. Alternatively, as glands mature, there may be an increase in the mesenchymal cells that contribute to the overall glandular nuclear counts, and thus reduce the fraction of cells that are GFP$^+$. However, when we quantified the percentage of SMG cells that were reactive with a pan-cytokeratin antibody, this percentage was not significantly different between 7-day-old (92.2 ± 2.4%) and 21-day-old (95.7 ± 1.9%) tracheas (Figure E4). For these reasons, we favor the former hypothesis that untraced glandular progenitors (either lineage-positive or lineage-negative)

preferentially expand later during gland development.

MEC Progenitors Give Rise to Multiple Cell Types during SMG Development

The findings of *ACTA2* lineage-labeled $GFP^+\alpha SMA^-$ cell types within developing SMGs suggests MECs can differentiate into phenotypically distinct cell types. To define these cell types, we colocalized the GFP lineage trace with markers of duct cells (Trop2), serous cells (lysozyme and *Dolichos biflorus* agglutinin [DBA] lectin), and mucus-producing cells (*Ulex europaeus* agglutinin I [UEA-1] lectin). UEA-1 has been previously shown to react with Muc5AC (37). In adult SMGs, DBA and UEA-1 react with two distinct cellular compartments that morphologically appear to be serous and mucous tubules (Figure E5). These phenotyping studies demonstrated the existence of GFP^+lysozyme$^+$ (Figure 5A) and GFP^+DBA^+ (Figure 5B) cell types consistent with the lineage marking of serous tubules. Similarly, GFP^+ tubules also reacted with UEA-1, consistent with mucous tubules (Figure 5C). A third less frequent lineage-tagged population of cells within SMGs was duct cells reactive with Trop2 (Figure 5D). Overall, these findings support the notion that MECs give rise to multiple distinct cellular populations during SMG development.

As one might expect, some of these serous and mucous tubules with a GFP^+ phenotype appeared clonal in origin (Figures 5A and 5C), suggesting an MEC progenitor had committed to form multiple cells within these tubules during development. Interestingly, not all GFP^+ cells were $tdTomato^-$ (Figure 5), however, it should be noted that the transgenic animals used were homozygous for the ROSA-TG locus. The finding of $GFP^+tdTomato^+$ cells supports the morphometric quantification that the lineage tracing efficiency was not complete using a single injection of tamoxifen (Figure 4C). Using this feature of incomplete Cre-mediated activation of GFP expression on the homozygous ROSA-TG background, we searched for evidence of clone-like tubules in 21-day-old mice pulsed with tamoxifen at birth. Although examples of lineage-positive cell clusters within tubules were found with either $GFP^+tdTomato^+$ or $GFP^+tdTomato^-$ phenotypes (Figure E6), tubules still retained some mixing of various reporter phenotypes. Thus, although MEC progenitors likely expand clonally within their local environment during gland development, it remains unclear whether entire tubules are clonally derived. Further experiments using a confetti reporter would be needed to quantitatively assess the extent to which this occurs during morphogenesis of glandular tubules.

MEC Lineage-Positive and Lineage-Negative Progenitors Both Contribute to Gland Development

Fate mapping using lineage-restricted Cre-drivers comes with caveats. The most critical caveats are specificity of the promoters used to lineage-trace the target cell type and lineage tracing efficiency (38, 39). To this end, we sought to validate our findings with a second *MYH11*-Cre^{ERT2} Cre-driver that efficiently marks MECs in adult SMGs (Figures E7A and E7B). Single tamoxifen dosing at birth in *MYH11*-Cre^{ERT2}:ROSA-TG mice gave rise to similar results as those observed in *ACTA2*-Cre^{ERT2}:ROSA-TG mice. At 21 days postinduction, there were significant numbers of SMMHC-positive lineage-traced MECs, as well as SMMHC-negative lineage-traced cells that clustered in tubules and acini (Figures E7C and E7D).

To determine the lineage tracing efficiency and maximal contribution of lineage-positive progenitors to non-MEC lineages within 21-day SMGs, we performed gavage dosing of tamoxifen every other day from birth to 18 days of age, using both the *ACTA2*-Cre^{ERT2}:ROSA-TG and *MYH11*-Cre^{ERT2}:ROSA-TG lines (Figures 6A and 6E). Morphometric analysis of 21-day SMGs for GFP and αSMA or SMMHC expression demonstrated that 94.2 ± 0.8% of αSMA^+ cells expressed GFP in *ACTA2*-Cre^{ERT2}:ROSA-TG mice and similarly, 95.5 ± 1.7% of $SMMHC^+$ cells expressed GFP in *MYH11*-Cre^{ERT2}:ROSA-TG mice. Thus, using this serial induction protocol, the lineage tracing efficiency was ∼ 95% using both Cre-drivers. As expected, this serial induction protocol gave rise to a larger percentage of SMG cells that were GFP^+ at 21 days (∼60% for both Cre-drivers) (Figure 6I) as compared with the ∼20% GFP^+ cells observed in mice labeled once at birth (Figure 4I). Importantly, the percentage of SMG lineage-traced GFP+ cells that were αSMA^- or $SMMHC^-$ was ∼50% for both Cre-drivers (Figure 6K), a value significantly higher than that observed after a single dose of tamoxifen at birth, using the *ACTA2*-Cre^{ERT2} driver (∼33%; $P < 0.0001$ using Student's *t* test) (Figure 4E).

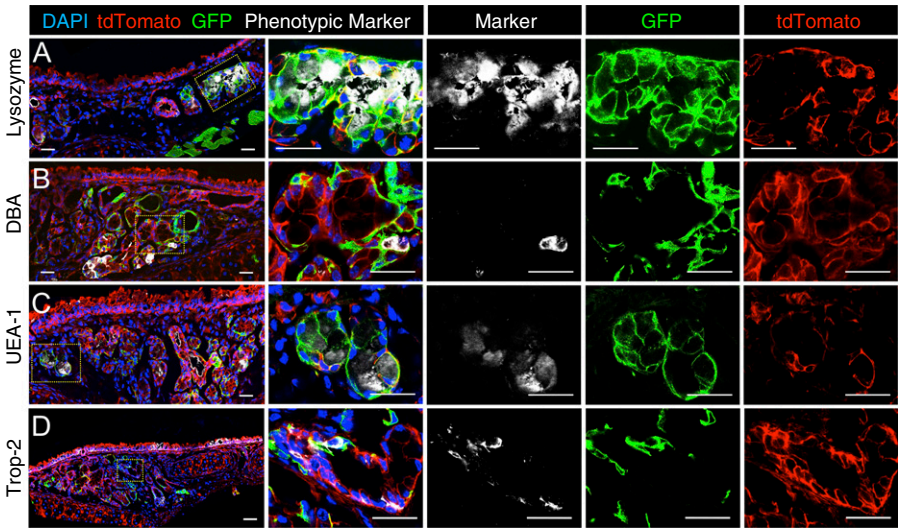

Figure 5. *ACTA2*-Cre^{ERT2} lineage-traced myoepithelial progenitors give rise to other submucosal gland cell types. *ACTA2*-Cre^{ERT2}:ROSA-TG mice were induced on the day of birth, and 21-day-old tracheal samples were then immunofluorescently stained with each of the indicated cellular markers, GFP, and tdTomato. DAPI was used to mark nuclei. (*A*) Lysozyme staining was used to identify serous cells. (*B*) *Dolichos biflorus* agglutinin (DBA) lectin staining was also used to identify serous cells. (*C*) *Ulex europaeus* agglutinin I (UEA-1) lectin staining was used to identify mucin within glandular mucous tubules. (*D*) Tumor-associated calcium signal transducer 2 (Trop-2) staining was used to identify duct cells. The *boxed region* in the main *left panel* is enlarged to the right as multi- and single-channel images. *Scale bars*: 25 μm.

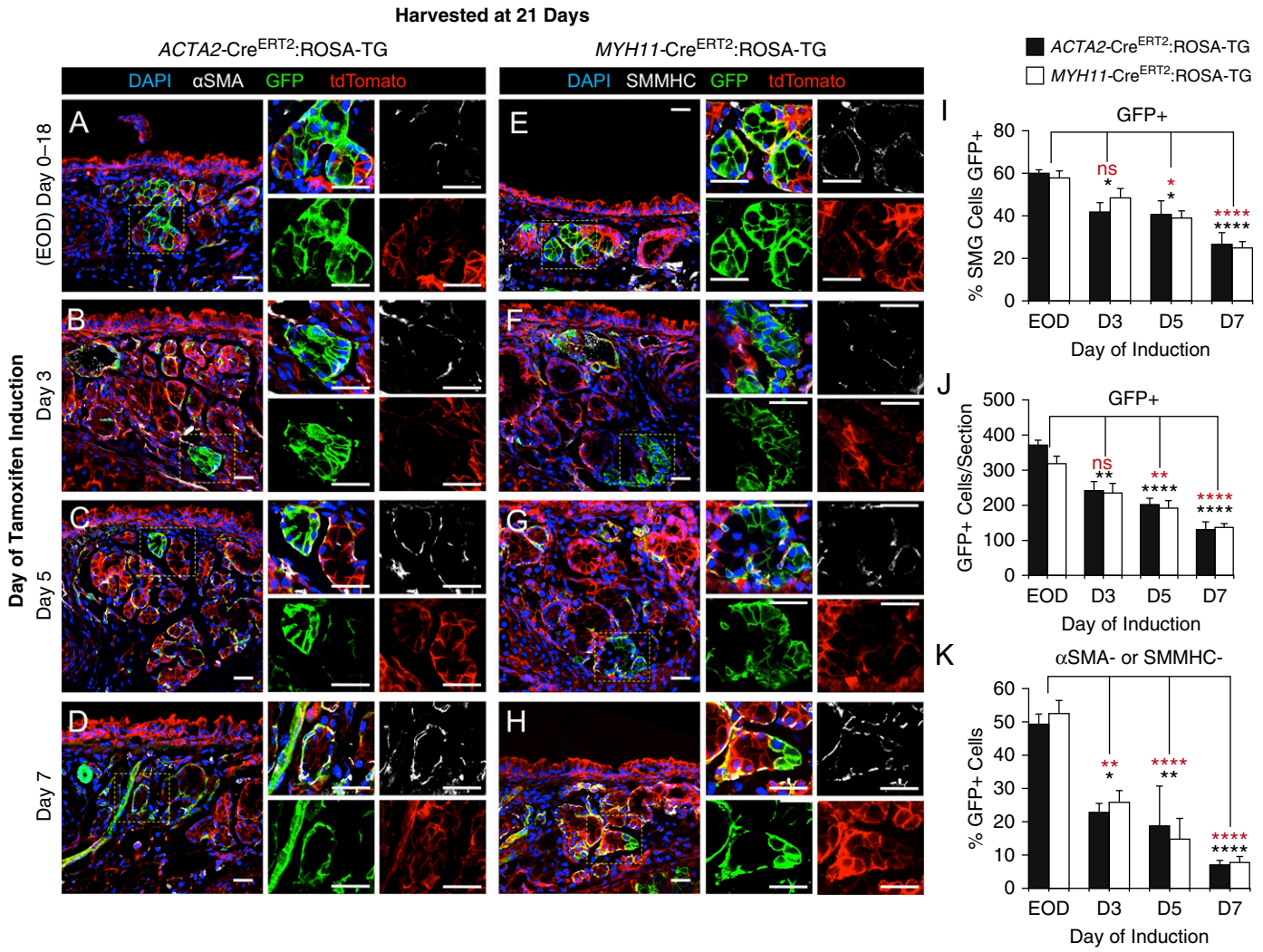

Figure 6. Lineage tracing of *ACTA2*-Cre^{ERT2} and smooth muscle myosin heavy chain 11 (*MYH11*)-Cre^{ERT2} labeled myoepithelial cells at various points after birth. *ACTA2*-Cre^{ERT2}:ROSA-TG and *MYH11*-Cre^{ERT2}:ROSA-TG mice were induced with tamoxifen by gavage every other day (EOD) from birth to 18 days or by a single intraperitoneal injection of tamoxifen on Days 3, 5, or 7 after birth. Tracheas were then harvested at 21 days and immunofluorescently stained for SMMHC, αSMA, GFP, and/or tdTomato, as indicated. DAPI was used to mark nuclei. (*A–D*) Representative low-power images of SMGs from *ACTA2*-Cre^{ERT2}:ROSA-TG mice with higher-power merged and single-channel images of the boxed region on the *right*. (*E–H*) Representative low-power images of SMGs from *MYH11*-Cre^{ERT2}:ROSA-TG mice are shown with higher-power merged and single-channel images of the boxed region on the right. (*I–K*) Morphometric analysis of the studies in (*A–H*) showing (*I*) the percentage of SMG cells staining GFP$^+$, (*J*) the number of GFP$^+$ cells per section, and (*K*) the percentage of GFP$^+$ glandular cells that did not express αSMA or SMMHC. Data depict the mean ± SEM of $n = 5–7$ mice evaluated. Asterisks denote significance levels using two-way ANOVA with Bonferroni's multiple comparison post-test: *$P < 0.05$; **$P < 0.01$; and ****$P < 0.0001$. ns, not significant. Significance marks compare the EOD condition to each single-pulse conditions for *ACTA2*-Cre^{ERT2}:ROSA-TG (*black text*) and *MYH11*-Cre^{ERT2}: ROSA-TG (*red text*) mice. *Scale bars*: 25 μm.

These findings suggest that multipotent lineage-positive MECs and lineage-negative glandular progenitors both contribute to non-MEC cellular compartments during glandular development.

To narrow down the window in which multipotent MECs are born during gland development, we also performed timed single-dose pulse inductions with tamoxifen in *ACTA2*-Cre^{ERT2}:ROSA-TG and *MYH11*-Cre^{ERT2}:ROSA-TG mice at 3, 5, or 7 days of age and evaluated the contribution of lineage-positive cells to SMG development at 21 days (Figures 6B–6D and 6F–6H). In most measurements quantified with both Cre-drivers, the every-other-day dosing of tamoxifen was significantly greater than single dosing at 3, 5, and 7 days for the percentage of GFP$^+$ SMG cells (Figure 6I), total number of GFP$^+$ cells per section (Figure 6J), and the percentage of GFP$^+$ cells that were αSMA$^-$ or SMMHC$^-$ (Figure 6K). Importantly, there was no significant difference in the quantification of these three endpoints between the two Cre-drivers. Although the percentage of lineage-positive cells that adopted a αSMA$^-$ or SMMHC$^-$ phenotype was not significantly different between Day 3 and 5-day induction groups, comparison of Day 3 to Day 7 induction demonstrated an approximately threefold significant decline in this cellular phenotype ($P < 0.001$ for both Cre-drivers, by Student's

t test) (Figure 6K). Furthermore, the sum of the percentage of GFP$^+$ cells that were αSMA$^-$ or SMMHC$^-$ for 3-, 5-, and 7-day pulse induction points was ~48% for both Cre-drivers (Figure 6K). This number was extremely close to the 50% achieved for this cellular phenotype, using every-other-day induction for 18 days (Figure 6K). Thus, we conclude that the majority of multipotent MEC progenitors are born during the 3–7-day postnatal period.

Discussion

MECs have been proposed to be potential progenitor cells of many glandular organs, including the mammary gland (25, 26, 40, 41), salivary gland (42), and lacrimal gland (28, 29). However, even in the mammary gland, the most extensively studied of these organs, a debate remains as to whether basal cell-like MECs are unipotent or multipotent (25, 26, 40). Much of the debate revolves around discrepancies between lineage tracing studies *in vivo* and *ex vivo*, using transplantation assays with isolated cell populations. For example, two studies demonstrate that mammary MECs and luminal cells are long-lived lineage-restricted progenitors during development, puberty, and pregnancy; however, transplantation assays with isolated mammary MECs have the capacity to self-renew and form whole mammary glands, whereas isolated luminal cells do not have this capacity (26, 40). In contrast, Rios and colleagues demonstrated, using lineage tracing clonal analysis, that a subset of mammary MEC progenitors has the capacity to differentiate into luminal cells during development (25). Similar to this later report, our findings demonstrate that early-born MECs can commit to forming multiple cell types during development of airway SMGs.

Using both αSMA and SMMHC MEC markers (Figure 1) and *ACTA2*-Cre^{ERT2} lineage tracing (Figure 2), MECs first emerge after placode formation during the elongation phase when invading SMG tubules form lumens. Based on the design of our initial lineage tracing studies (i.e., single induction at birth), our data suggest that ~50% of self-renewing glandular MECs emerge during the first few days of the neonatal period. This calculation is based on ~50% lineage tracing efficiency at 3 days and the finding of fewer (~25%) lineage-tagged αSMA$^+$ cells by 21 days (Figure 4C). These lineage-positive cells and their descendents expanded 10-fold between 3 and 21 days of SMG development (Figure 4H; $P < 0.001$). Although it is difficult to estimate the bioavailability of tamoxifen in newborn mice after a single injection at ~200 mg/kg (intraperitoneally), based on a 12-hour half-life of tamoxifen in serum after oral dosing to adult mice (43), we assume, at the high dose given in these studies, that it persists for 2–3 days. Interestingly, the percentage of 21-day αSMA$^+$ or SMMHC$^+$ glandular cells that were also GFP$^+$ after a single tamoxifen pulse at 3, 5, or 7 days of age in *ACTA2*-Cre^{ERT2}:ROSA-TG or *MYH11*-Cre^{ERT2}:ROSA-TG mice, respectively, was not significantly different (ranging from 72% to 83% for *ACTA2*-Cre^{ERT2} and 70% to 74% for *MYH11*-Cre^{ERT2} and averaging 75.0 ± 1.9% for the six groups). This lineage-labeling efficiency of MECs (75.0 ± 1.9%) using both Cre-drivers was approximately threefold higher than that after a single tamoxifen injection at birth in *ACTA2*-Cre^{ERT2}:ROSA-TG

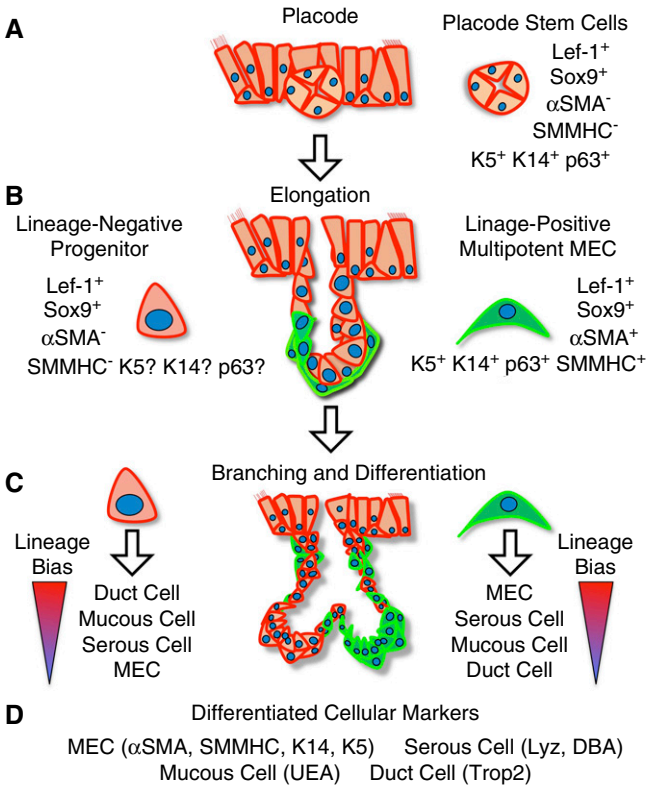

Figure 7. Model of the lineage hierarchy for the developing airway submucosal gland. (*A*) Stem cells of the primordial gland placode express basal cell markers (CK5, CK14, p63), but lack myoepithelial cell (MEC) markers (αSMA and SMMHC). Two transcription factors, lymphoid enhancer binding factor-1 (Lef-1) and SRY-box 9 (Sox9), are also highly expressed in the stem cells of the primordial gland placode. (*B*) During the elongation phase, the first lineage-positive MECs (αSMA$^+$, SMMHC$^+$) emerge at the tips of the elongating tubules. Lineage tracing studies suggest that the MECs born during the 3–7-day window after birth are multipotent and retain Lef-1 and Sox9 expression, as well as other basal cell phenotypes (CK5$^+$, CK14$^+$, and p63$^+$). However, these data also support the existence of a second lineage-negative progenitor (i.e., not of MEC lineage, αSMA$^-$, SMMHC$^-$) that contributes cells to the developing SMG. These lineage-negative progenitors likely also express Lef-1 and Sox9, as nearly all cells of the tubule express these transcription factors at this stage. However, because expression of basal cell markers during the elongation phase is not uniform, it is unclear whether lineage-negative progenitors express CK5 and/or CK14. (*C*) During branching and differentiation phases of SMG development, multipotent MECs can give rise to new MECs and differentiate into serous cells, mucous cells, and ductal cells. Although the lineage hierarchy of MEC progenitors remains unclear, timed pulse induction studies after birth suggest that both multipotent and unipotent MECs likely exist. Lineage-negative progenitors appear to have a lineage bias for differentiation into ductal cells and mucous cells, but less frequently differentiate into serous cells and MECs. The *inverted triangles* schematically show the relative lineage bias for differentiation of each progenitor population (*red*, most abundant; *blue*, least abundant). (*D*) Differentiation markers used in this study to define various cell types.

mice (24.7 ± 4.9%) (Figure 4C). These findings suggest that a self-renewing unipotent MEC progenitor likely emerges by ~3–4 days after birth and may contribute to the majority of MECs in the 21-day gland.

The most conclusive evidence that a subset of MECs formed early during gland development are multipotent progenitors comes from the finding that lineage-positive αSMA-negative cells rose fivefold between 3 to 21 days postinduction at birth (Figure 4E). Interestingly, lineage-positive cells and their descendents constituted 50% of SMG tubular epithelia at 7 days postinduction, but this percentage dropped to 22% by 21 days (Figure 4I), despite a 3.2-fold rise in the total number of GFP^+ glandular cells during this period (Figure 4H). Several potential explanations may account for these two seemingly disparate results. First, untraced MEC progenitors that emerge later during SMG development may contribute to a larger proportion of glandular epithelia. This would imply that the lineage-positive MECs born early during morphogenesis have a limited capacity for self-renewal and differentiation into other glandular cell types. Second, lineage-negative (non-MEC) progenitors may expand to form specific cellular compartments later during SMG development. Studies using multiple serial inductions and timed single-dose induction of *ACTA2*-Cre^{ERT2} and *MYH11*-Cre^{ERT2} driver mice suggest the later hypothesis is likely correct. The maximal contribution of lineage-positive MECs to all SMG cells was ~60% for both Cre drivers when mice were induced every other day for 18 days (Figure 6I). Given that the lineage tracing efficiency in this multiple-dose study was ~95% of αSMA^+ and $SMMHC^+$ MECs, these findings demonstrate that both lineage-positive and lineage-negative progenitors contribute to SMG development. Timed single-dose tamoxifen injections also suggest that the window for birth of multipotent MECs is highest between 3 and 7 days after birth (Figure 6K), assuming tamoxifen bioavailability from 3- and 5-day injection spans that period. Although we did not perform single-induction points past 7 days of age, one would predict that very few lineage-positive cells would have an αSMA^- and $SMMHC^-$ phenotype when induction is performed past 9 days of age. These findings warrant further investigation to define the hierarchy of MEC and non-MEC glandular progenitors during gland morphogenesis.

Our findings provide evidence that *ACTA2*-expressing MECs born early during airway SMG morphogenesis are a self-renewal progenitor capable of contributing to serous cell lineages (Figure 5). However, other less abundant lineage-tagged cell types included Trop2-expressing and mucus-producing cells. Thus, one interpretation of these findings could be that lineage-positive multipotent MECs have a bias toward MEC and serous cell lineages, whereas lineage-negative glandular progenitors may primarily contribute to duct- and mucus-producing cellular lineages (Figure 7). However, it should be noted that mucous tubules appear to not be fully formed by 21 days compared with adult SMGs (Figure E5). $Trop2^+$ cells of the gland duct have been demonstrated to have multipotent capacity for differentiation into surface airway epithelial cell types after injury (12). Whether glandular MECs are precursors to duct cells in adult mice, and thus sit at the apex of the glandular progenitor cell hierarchy, remains to be determined. The formation of lineage-tagged serous and mucous cell clusters within tubules (Figures 5A and 5C and Figure E6) suggests that MEC-derived progenitors may commit toward various lineages and expand locally during SMG morphogenesis. However, it remains unclear whether MECs can directly differentiate into various glandular cell types or, rather, are directed toward a lineage-committed progenitor cell that lacks αSMA expression. The appearance of tightly packed lineage-tagged cell clusters that lack αSMA expression lends support to the later hypothesis (Figures 2Ciii, Dv, and Eviii; Figure 4B, upper; Figure E8). These tight cellular clusters that lack tubular structure are reminiscent of $CK5^+$ pods in the distal lung after severe lung injuries (44, 45). These $CK5^+$ pods have been suggested to be composed of multipotent progenitors capable of distal lung repair after necrotizing influenza infection. Further phenotyping and additional lineage tracing studies are needed to definitively answer these questions, as they pertain to multipotent MECs.

In summary, we have shown using lineage tracing that multipotent MECs are born very early during airway gland morphogenesis and that these progenitor cells have the ability to form multiple luminal cell types that lack expression of MEC markers (Figure 7). Our data are also consistent with a self-renewing population of unipotent MECs that emerges during this same period. Importantly, our findings also support a lineage-independent progenitor cell population that is equally important for gland morphogenesis (Figure 7). Whether MECs of adult SMGs retain a multipotent capacity for differentiation during normal cellular turnover and disease-based glandular hypertrophy remains unclear. However, findings from this study suggest that further investigation into whether adult MECs have multipotent stem cell characteristics after airway injury is warranted. ■

Author disclosures are available with the text of this article at www.atsjournals.org.

Acknowledgment: The authors thank Dr. Paul Herring for providing the Tg(Acta2-cre/ERT2) 51Pcn (*ACTA2-Cre*^{ERT2}) mice.

References

1. Dajani R, Zhang Y, Taft PJ, Travis SM, Starner TD, Olsen A, Zabner J, Welsh MJ, Engelhardt JF. Lysozyme secretion by submucosal glands protects the airway from bacterial infection. *Am J Respir Cell Mol Biol* 2005;32: 548–552.
2. Wine JJ, Joo NS. Submucosal glands and airway defense. *Proc Am Thorac Soc* 2004;1:47–53.
3. Borthwick DW, Shahbazian M, Krantz QT, Dorin JR, Randell SH. Evidence for stem-cell niches in the tracheal epithelium. *Am J Respir Cell Mol Biol* 2001;24:662–670.
4. Hegab AE, Ha VL, Darmawan DO, Gilbert JL, Ooi AT, Attiga YS, Bisht B, Nickerson DW, Gomperts BN. Isolation and in vitro characterization of basal and submucosal gland duct stem/progenitor cells from human proximal airways. *Stem Cells Transl Med* 2012;1:719–724.
5. Hegab AE, Ha VL, Gilbert JL, Zhang KX, Malkoski SP, Chon AT, Darmawan DO, Bisht B, Ooi AT, Pellegrini M, *et al*. Novel stem/progenitor cell population from murine tracheal submucosal gland ducts with multipotent regenerative potential. *Stem Cells* 2011;29:1283–1293.
6. Lynch TJ, Anderson PJ, Xie W, Crooke AK, Liu X, Tyler SR, Luo M, Kusner DM, Zhang Y, Neff T, *et al*. Wnt signaling regulates airway epithelial stem cells in adult murine submucosal glands. *Stem Cells* 2016;34:2758–2771.

7. Lynch TJ, Engelhardt JF. Progenitor cells in proximal airway epithelial development and regeneration. *J Cell Biochem* 2014;115:1637–1645.
8. Jeffery PK. Remodeling in asthma and chronic obstructive lung disease. *Am J Respir Crit Care Med* 2001;164:S28–S38.
9. Dunnill MS, Massarella GR, Anderson JA. A comparison of the quantitative anatomy of the bronchi in normal subjects, in status asthmaticus, in chronic bronchitis, and in emphysema. *Thorax* 1969; 24:176–179.
10. Xie W, Fisher JT, Lynch TJ, Luo M, Evans TI, Neff TL, Zhou W, Zhang Y, Ou Y, Bunnett NW, *et al*. CGRP induction in cystic fibrosis airways alters the submucosal gland progenitor cell niche in mice. *J Clin Invest* 2011;121:3144–3158.
11. Wansleeben C, Barkauskas CE, Rock JR, Hogan BL. Stem cells of the adult lung: their development and role in homeostasis, regeneration, and disease. *Wiley Interdiscip Rev Dev Biol* 2013;2:131–148.
12. Hegab AE, Nickerson DW, Ha VL, Darmawan DO, Gomperts BN. Repair and regeneration of tracheal surface epithelium and submucosal glands in a mouse model of hypoxic-ischemic injury. *Respirology* 2012;17:1101–1113.
13. Engelhardt JF. Stem cell niches in the mouse airway. *Am J Respir Cell Mol Biol* 2001;24:649–652.
14. Liu X, Driskell RR, Engelhardt JF. Stem cells in the lung. *Methods Enzymol* 2006;419:285–321.
15. Rawlins EL, Hogan BL. Ciliated epithelial cell lifespan in the mouse trachea and lung. *Am J Physiol Lung Cell Mol Physiol* 2008;295: L231–L234.
16. Liu X, Driskell RR, Engelhardt JF. Airway glandular development and stem cells. *Curr Top Dev Biol* 2004;64:33–56.
17. Liu X, Engelhardt JF. The glandular stem/progenitor cell niche in airway development and repair. *Proc Am Thorac Soc* 2008;5:682–688.
18. Driskell RR, Goodheart M, Neff T, Liu X, Luo M, Moothart C, Sigmund CD, Hosokawa R, Chai Y, Engelhardt JF. Wnt3a regulates Lef-1 expression during airway submucosal gland morphogenesis. *Dev Biol* 2007;305:90–102.
19. Driskell RR, Liu X, Luo M, Filali M, Zhou W, Abbott D, Cheng N, Moothart C, Sigmund CD, Engelhardt JF. Wnt-responsive element controls Lef-1 promoter expression during submucosal gland morphogenesis. *Am J Physiol Lung Cell Mol Physiol* 2004;287: L752–L763.
20. Duan D, Sehgal A, Yao J, Engelhardt JF. Lef1 transcription factor expression defines airway progenitor cell targets for in utero gene therapy of submucosal gland in cystic fibrosis. *Am J Respir Cell Mol Biol* 1998;18:750–758.
21. Duan D, Yue Y, Zhou W, Labed B, Ritchie TC, Grosschedl R, Engelhardt JF. Submucosal gland development in the airway is controlled by lymphoid enhancer binding factor 1 (LEF1). *Development* 1999;126:4441–4453.
22. Liu X, Luo M, Xie W, Wells JM, Goodheart MJ, Engelhardt JF. Sox17 modulates Wnt3A/beta-catenin-mediated transcriptional activation of the Lef-1 promoter. *Am J Physiol Lung Cell Mol Physiol* 2010;299: L694–L710.
23. Xie W, Lynch TJ, Liu X, Tyler SR, Yu S, Zhou X, Luo M, Kusner DM, Sun X, Yi Y, *et al*. Sox2 modulates Lef-1 expression during airway submucosal gland development. *Am J Physiol Lung Cell Mol Physiol* 2014;306:L645–L660.
24. Martignani E, Cravero D, Miretti S, Accornero P, Baratta M. Clonogenic assay allows for selection of a primitive mammary epithelial cell population in bovine. *Exp Cell Res* 2015;338:245–250.
25. Rios AC, Fu NY, Lindeman GJ, Visvader JE. In situ identification of bipotent stem cells in the mammary gland. *Nature* 2014;506: 322–327.
26. Prater MD, Petit V, Alasdair Russell I, Giraddi RR, Shehata M, Menon S, Schulte R, Kalajzic I, Rath N, Olson MF, *et al*. Mammary stem cells have myoepithelial cell properties. *Nat Cell Biol* 2014;16(10):942–950.
27. Regan J, Smalley M. Prospective isolation and functional analysis of stem and differentiated cells from the mouse mammary gland. *Stem Cell Rev* 2007;3:124–136.
28. Makarenkova HP, Dartt DA. Myoepithelial cells: their origin and function in lacrimal gland morphogenesis, homeostasis, and repair. *Curr Mol Biol Rep* 2015;1:115–123.
29. Shatos MA, Haugaard-Kedstrom L, Hodges RR, Dartt DA. Isolation and characterization of progenitor cells in uninjured, adult rat lacrimal gland. *Invest Ophthalmol Vis Sci* 2012;53:2749–2759.
30. Muzumdar MD, Tasic B, Miyamichi K, Li L, Luo L. A global double-fluorescent Cre reporter mouse. *Genesis* 2007;45:593–605.
31. Wirth A, Benyó Z, Lukasova M, Leutgeb B, Wettschureck N, Gorbey S, Orsy P, Horváth B, Maser-Gluth C, Greiner E, *et al*. G12-G13-LARG-mediated signaling in vascular smooth muscle is required for salt-induced hypertension. *Nat Med* 2008;14:64–68.
32. Wendling O, Bornert JM, Chambon P, Metzger D. Efficient temporally-controlled targeted mutagenesis in smooth muscle cells of the adult mouse. *Genesis* 2009;47:14–18.
33. Boras-Granic K, Chang H, Grosschedl R, Hamel PA. Lef1 is required for the transition of Wnt signaling from mesenchymal to epithelial cells in the mouse embryonic mammary gland. *Dev Biol* 2006;295:219–231.
34. van Genderen C, Okamura RM, Fariñas I, Quo RG, Parslow TG, Bruhn L, Grosschedl R. Development of several organs that require inductive epithelial-mesenchymal interactions is impaired in LEF-1-deficient mice. *Genes Dev* 1994;8:2691–2703.
35. Malhotra GK, Zhao X, Edwards E, Kopp JL, Naramura M, Sander M, Band H, Band V. The role of Sox9 in mouse mammary gland development and maintenance of mammary stem and luminal progenitor cells. *BMC Dev Biol* 2014;14:47.
36. Rock JR, Onaitis MW, Rawlins EL, Lu Y, Clark CP, Xue Y, Randell SH, Hogan BL. Basal cells as stem cells of the mouse trachea and human airway epithelium. *Proc Natl Acad Sci USA* 2009;106:12771–12775.
37. Pardo-Saganta A, Law BM, Gonzalez-Celeiro M, Vinarsky V, Rajagopal J. Ciliated cells of pseudostratified airway epithelium do not become mucous cells after ovalbumin challenge. *Am J Respir Cell Mol Biol* 2013;48:364–373.
38. Kretzschmar K, Watt FM. Lineage tracing. *Cell* 2012;148:33–45.
39. Rios AC, Fu NY, Cursons J, Lindeman GJ, Visvader JE. The complexities and caveats of lineage tracing in the mammary gland. *Breast Cancer Res* 2016;18:116.
40. Van Keymeulen A, Rocha AS, Ousset M, Beck B, Bouvencourt G, Rock J, Sharma N, Dekoninck S, Blanpain C. Distinct stem cells contribute to mammary gland development and maintenance. *Nature* 2011;479:189–193.
41. Visvader JE, Stingl J. Mammary stem cells and the differentiation hierarchy: current status and perspectives. *Genes Dev* 2014;28: 1143–1158.
42. Takahashi S, Shinzato K, Domon T, Yamamoto T, Wakita M. Mitotic proliferation of myoepithelial cells during regeneration of atrophied rat submandibular glands after duct ligation. *J Oral Pathol Med* 2004; 33:430–434.
43. Robinson SP, Langan-Fahey SM, Johnson DA, Jordan VC. Metabolites, pharmacodynamics, and pharmacokinetics of tamoxifen in rats and mice compared to the breast cancer patient. *Drug Metab Dispos* 1991;19:36–43.
44. Vaughan AE, Brumwell AN, Xi Y, Gotts JE, Brownfield DG, Treutlein B, Tan K, Tan V, Liu FC, Looney MR, *et al*. Lineage-negative progenitors mobilize to regenerate lung epithelium after major injury. *Nature* 2015;517:621–625.
45. Zuo W, Zhang T, Wu DZ, Guan SP, Liew AA, Yamamoto Y, Wang X, Lim SJ, Vincent M, Lessard M, *et al*. p63(+)Krt5(+) distal airway stem cells are essential for lung regeneration. *Nature* 2015;517:616–620.